J Comput Aided Mol Des (2007) 21:641–648
DOI 10.1007/s10822-007-9147-6

Computational study on mechanism of G-quartet oligonucleotide T40214 selectively targeting Stat3

Qiqing Zhu · Naijie Jing

Received: 31 January 2007 / Accepted: 1 November 2007 / Published online: 22 November 2007

Abstract The mounting evidences have shown that signal transducer and activator of transcription 3 (Stat3) is a critical target for cancer therapy. Recently, we developed a G-quartet oligonucleotide T40214 as a novel and potent Stat3 inhibitor. T40214 specifically inhibited DNA-binding activity of Stat3 and significantly suppressed the growth of many tumor xenografts in nude mice. To determine the mechanism of GQ-ODNs selectively targeting Stat3, we established a 3D model of complex T40214/p-Stat3 dimer based on experimental evidences. The binding site of T40214 within Stat3 dimer was determined by statistical docking analysis. The results indicated that T40214 strongly interacted within the region from residue E638 through E652 of Stat3 dimer. The binding model refined by *Hex* docking disclosed that T40214 binds to SH2 domain of Stat3 and forms H-bonds with residues Q643, Q644, N646, and N647, which are critical for the binding interaction. The 3D models also suggested that T40214 inhibits Stat3 activity through disrupting the binding interaction between Stat3 dimer and DNA duplex for transcription. Our computational studies provided a platform for future structure-based drug design of novel Stat3 inhibitors.

Keywords Stat3 · Stat1 · Molecular docking · T40214 · GQ-ODN

Q. Zhu · N. Jing (✉)
Department of Medicine, Baylor College of Medicine, One Baylor Plaza, N1317.05, Houston, TX 77030, USA
e-mail: njing@bcm.tmc.edu

N. Jing
Cancer Center, Baylor College of Medicine, Houston, TX 77030, USA

Introduction

Signal transducer and activator of transcription 3 (Stat3) as a mediator participates in many cellular processes, e.g., differentiation, proliferation, cell survival, apoptosis, and angiogenesis [1–6]. Initially identified as a DNA binding activity within IL-6-stimulated hepatocytes, Stat3 is capable of selectively interacting with an enhancer element in the promoter region of acute-phase response genes [7–10]. Stat3 activation is essential to the growth and survival of cancer cells [11, 12] and it plays a critical role in oncogenic signaling through the up-regulation of genes encoding apoptosis inhibitors (Bcl-x_L, Mcl-1, and survivin), cell-cycle regulators (cyclin D1 and c-*myc*), and inducers of angiogenesis (VEGF) [13]. Stat3 has been found to be persistently activated in many human cancers (e.g., prostate, breast, lung, head and neck, and pancreas, etc.) [13, 14], so Stat3 is considered to be a critical molecular target for novel anti-cancer therapy.

When stimulated by cytokines [15, 16], Stat3 is activated upon phosphorylation in tyrosine residue Y705 [17]. The phosphorylated Stat3 (p-Stat3) then translocates into the nucleus, where it binds to enhancer sequence of target gene and forms a parallel dimer [18, 19]. Stat3 shares similar structure characteristics with other STAT proteins, including the N-terminal domain [20], the coiled-coil domain, the DNA-binding domain [21], the SH2 domain [22], the transactivation domain, and the carboxyl terminal domain. According to Stat3 function and its structure, there are several strategies to rationally design Stat3 inhibitor, including to (i) block receptor–ligand interaction by designing ligand competitor, e.g. design compounds to compete with IL-6 or EGF; (ii) block the residue of tyrosine 705 phosphorylation; (iii) inhibit the DNA binding of p-Stat3 by designing compounds to compete with the DNA

sequence; (iv) block the formation of activated p-Stat3 dimer; and (v) inhibit Stat3 transcription function in the nucleus by designing antisense sequence [11, 23]. In this article, we demonstrate that G-quartet oligonucleotide (GQ-ODN) T40214 inhibits Stat3 activity by disrupting its DNA binding ability.

Recently, we developed a series of GQ-ODNs as Stat3 inhibitors and they showed low micromolar IC_{50} potency against tumor-derived cell lines in vitro [24]. We also found that GQ-ODN T40214 as the most potent agent significantly suppressed the growth of prostate, breast, head and neck, and non-small cell lung cancer (NSCLC) tumors in nude mice xenograft models [25–27]. Our results indicate that GQ-ODN T40214 is a promising drug candidate for the treatment of human cancers by targeting Stat3. In order to determine the mechanism that GQ-ODN T40214 inhibits Stat3 activity and gain insight into this process, we established the 3D complex of T40214/p-Stat3 dimer by combining experimental results with computational technologies. Furthermore, Stat1 and Stat3 are closely related transcription factors with different effect on cell proliferation and apoptosis [28–30]—Stat1 plays a role in promoting apoptosis in cells, whereas Stat3 has an anti-apoptotic effect. Stat1 might enhance the activity of p53 pro-apoptotic transcription factor as well. So selectively inhibiting Stat3 rather than Stat1 is very important for the design of an effective Stat3 inhibitor. Our electrophoretic mobility shift assay (EMSA) data demonstrated that T40214 selectively inhibits Stat3 activity rather than Stat1; the selectivity of Stat3 *versus* Stat1 is more than 30-fold [26, 27]. To understand the mechanism of T40214 selectively targeting Stat3 and disclose useful information for structure-based design of Stat3 inhibitor, we demonstrated the structural differences of T40214-binding site between in Stat1 dimer and in Stat3 dimer by using sequence alignment and 3D-structure comparison. We also compared the detailed interactions based on 3D complexes of T40214/p-Stat1 and T40214/p-Stat3.

Materials and methods

Cell culture and DNA-binding assay

EMSA was used to measure DNA-binding activity of Stat3. Briefly, the human cancer cells HepG2 was stimulated with Interleukin-6 (IL-6) and cultured in DMEM medium containing 10% fetal bovine serum, 100 units/ml penicillin and 100 units/ml streptomycin. Cells were then washed with high-salt buffer and lysed by freezing and thawing 4–5 times on dry ice. Lysate was centrifuged at 12,000 rpm for 20 min at 4 ^{o}C to take the supernatant. The protein concentration in the supernatant was measured using Bradford Protein Assay at the wavelength of 595 nm. The cell proteins (5 μg) treated with or without GQ-ODN T40214 (7 μM) were incubated with 1 μl of ^{32}P-labeled DNA probe (hSIE) in binding buffer with 2 μg of poly-dIdC at room temperature for 15 min. Samples were loaded onto 5% polyacrylamide gel containing 0.25X TBE and 2.5% glycerol. The gel was run at 160–200 V for 2–3 h at room temperature, then dried and autoradiographed.

Western blot analysis

Western blot was employed to identify the influence of GQ-ODN on Stat3 phosphorylation. Non-small cell lung cancer (NSCLC) cells A549 were stimulated with IL-6 (25 ng/ml) for 30 min. Cells were then washed in serum-free medium and incubated with various concentrations (1.4–142 μM) of T40214/PEI mixtures for 24 h. Cytoplasmic extracts were prepared with cell lysis buffer and 30 μg of whole cell protein was loaded on 10% SDS-PAGE gel, transferred to a nitrocellulose membrane, blocked with 5% non-fat milk, and probed with specific antibody against Stat3 and p-Stat3. The bands were quantitated using Personal Densitometer Scanner (version 1.30) and ImageQuant software (version 3.3).

Structure preparation

Single-stranded G-rich oligonucleotide T30695 was identified as a G-quartet conformation in solution environment by NMR, CD, UV and melting point studies [31]. The 3D structure of T40214 was constructed by replacing bases of T30695. Employing the InsightII/Discover module with AMBER force field (Accelrys, Inc., San Diego, CA), local energy minimization was performed on the new bases before T40214 was fully optimized [32]. Conjugate gradient energy minimization was used to optimize geometry and energy convergence was set at 0.01 kal/mol. The intramolecular H-bonds required for G-quartet formation were maintained during all of geometry optimizations. Crystal structures of Stat1 dimer [19] (PDB ID: 1BF5) and Stat3 [18] (NDB ID: PD0028) dimer were obtained from the Protein Data Bank [33] and the Nucleic Acid Database [34], respectively.

Molecular docking

Molecular dockings were performed with GRAMM and *Hex* programs. Without setting any restriction, the first GRAMM docking of T40214 to p-Stat3 dimer was carried out at low-resolution (grid step 3.3 Å, angular interval for

rotation 30°) and the 1000 complex with lowest energy were collected to perform statistical analysis. The results from the statistical analysis are used to determine if T40214 dominantly binds in special area, which will be used as constrain in future docking studies. In statistical analyses, all of the amino acids within 5.0 Å of T40214 were defined as binding site residues and H-bonds between p-Stat3 dimer and T40214 were identified in accordance with geometric standards used by the InsightII/Viewer module. The second GRAMM docking was done at high-resolution (grid step 1.7 Å, angular interval for rotation 10°) and the lowest energy complex obtained from this docking was used as initial structure for *Hex* docking.

Hex docking was utilized to search possible binding model for T40214 [35]. Our *Hex* docking was restricted to the primary binding site identified by GRAMM docking. *Hex* docking selected full rotation as search mode (including rotation and translation), and the rotational step for both receptors and ligands was about 6.7°. T40214 was rotated 360° about an intermolecular axis in 128 increments of approximately 2.8°. All of the rotations were repeated at a stepsize of ±0.5 Å along the intermolecular axis from the starting point to 10 Å. The best 10,000 orientations from $N = 16$ scan phase (where N is the order of Fourier expansions) were further refined by combining higher order shape and electronic correlations at $N = 25$. Subsequently, the lowest energy 512 of the refined 10,000 orientations were saved and clustered to generate distinct docking orientations.

Sequence alignment and structural comparison

The amino acid sequences in the core structure (Stat1: residues 136 to 712 and Stat3: residues 136 to 716) were retrieved from the SWISS-PROT database [36]. Two sequences were aligned with ClustalW 1.82 program [37]. No further modification was undertaken during alignment. We compared 3D structures of Stat3 with Stat1 with the InsightII/Viewer module.

Results and discussion

Inhibition of Stat3 activity by T40214

We have developed GQ-ODNs as a new class of Stat3 inhibitors. The lead compound, GQ-ODN T40214, selectively inhibits DNA-binding activity of Stat3 ($IC_{50} = 5$ μM) in the several cancer cells and significantly suppresses the tumor growth in xenograft animal models [26, 27]. T40214, a G-rich oligonucleotide, forms a G-quartet DNA structure, in which two G-quartets in the middle and two G–C–G–C loop domains in the top and bottom (Fig. 1a, b) [24]. T40214 activity was determined using electrophoretic mobility shift assay (EMSA). To determine the mechanism of T40214 inhibiting Stat3 activity, we added T40214 (7 μM) to Stat3 samples in three ways: before or at the same time or after adding the probe DNA (hSIE) in the samples, respectively. The results (Fig. 1c) demonstrated that comparing with control (Lane 1), no inhibition was observed when T40214 added before or at the same time as the probe DNA (Lanes 2 and 3); however, strong inhibition was observed when T40214 added 15 min after the probe DNA (Lane 4).

The crystal structures demonstrated that conformation of STAT dimer depends on phosphorylation of tyrosine residue (e.g. Stat3 Tyr705) in SH2 domain and DNA duplex binding in DNA binding domain as well. For example, both unphosphorylated Stat5a [38] and unphosphorylated Stat1 [39] adopt an N-terminal to N-terminal anti-parallel conformation; phosphorylated dictyostelium STAT without bound DNA is a fully extended head to head dimer [40]; however, phosphorylated Stat3 with bound DNA shows a reciprocally parallel dimer [18]. Therefore, unphosphorylated Stat3 dimer will presents an N-terminal to N-terminal anti-parallel conformation; when Stat3 is phosphorylated but without DNA binding, it should form a fully extended head to head dimer; however, upon binding DNA duplex in

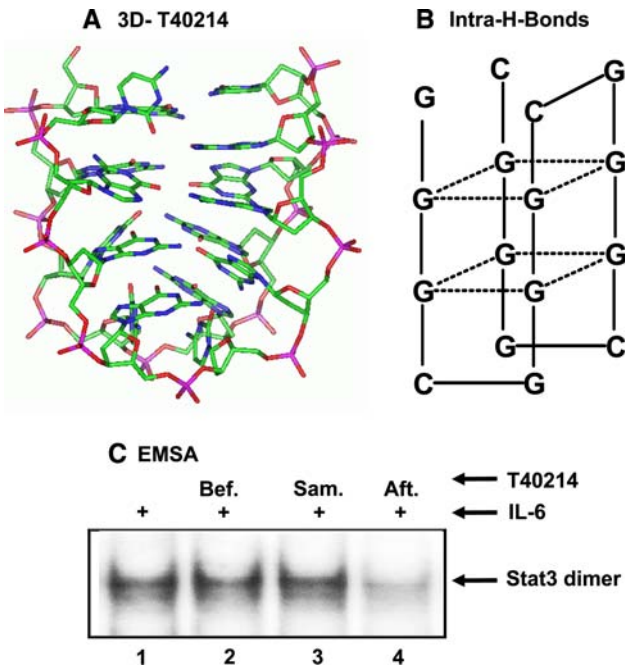

Fig. 1 GQ-ODN T40214 inhibits Stat3 activity. (**a**) 3D structure of GQ-ODN T40214. (**b**) Intra-H-bonds required for G-quartet conformation of T40214, indicated by dashed lines. (**c**) EMSA results of T40214 in IL-6- stimulated HepG2 cells, Lane 1 is a control sample (with hSIE only), Lanes 2, 3, and 4 show the T40214 efficacy on Stat3 DNA-binding activity when T40214 was added before, at the same time as, and after the DNA duplex (hSIE), respectively

DNA binding domain, the structure of phosphorylated Stat3 dimer will transform to a reciprocally parallel conformation. Our EMSA results indicated that T40214 showed inhibition on DNA-binding activity of Stat3 only when the probe DNA bound within p-Stat3 dimer, suggesting that T40214 blocks Stat3 activity by targeting the reciprocally parallel conformation, which is formed by the binding of probe DNA duplex. This observation is the experimental basis for us to select the reciprocally parallel p-Stat3 dimer [18] as receptor structure for our further docking studies.

Determination of T40214 binding site in Stat3 dimer

We employed statistics-based docking strategy to identify binding site for T40214. Without setting any restriction, T40214 was docked into crystal structure of p-Stat3 dimer [18] and a total of 1000 complexes of T40214/p-Stat3 dimer were collected for statistical analysis. In each complex, all of residues within 5.0 Å of T40214 were identified as possible binding site residues. The possibility for each amino acid interacting with T40214 was analyzed and the amino acids with high possibility will construct a potential binding site for T40214. The possibility versus Stat3 amino acid residue was plotted in Fig. 2a. As showed in Fig. 2a, the binding site residues dominantly distributed in four areas: (i) D566 to L579, (ii) R609 to T620, (iii) E638 to E652, and (iv) A702 to F710. The possibilities of T40214 binding within these four areas were estimated as 8%, 9%, 37%, and 14%, respectively. Therefore, the region from E638 to E652 with the highest possibility (37%) was predicted as a potential binding site for T40214. Also, the statistic analysis showed that Q643, Q644, N646, and N647 are critical residues to interact with T40214.

H-bonds plays very important role in governing interaction between proteins and DNA. We also statistically analyzed the total 15,935 H-bonds from the 1000 complexes of T40214/p-Stat3 dimer based on the geometric criteria used in the Insight II program. The histogram of H-bond number versus amino acid of Stat3 demonstrated that H-bonds mainly distributed in the same four areas of Stat3 dimer: (i) D566 to L579; (ii) R609 to T620; (iii) E638 to E652; and (iv) A702 to F710; and the percentages of H-bond distribution among these four areas were 7%, 9%, 39%, and 12%, respectively. Residues Q643, Q644, N646, and N647 have the greatest potential to form H-bonds with T40214.

Mechanism of T40214 blocking Stat3 activation

To establish 3D model of T40214/p-Stat3 dimer for structure-based drug design, we performed 6D-level *Hex* docking by using the core structure of p-Stat3 dimer

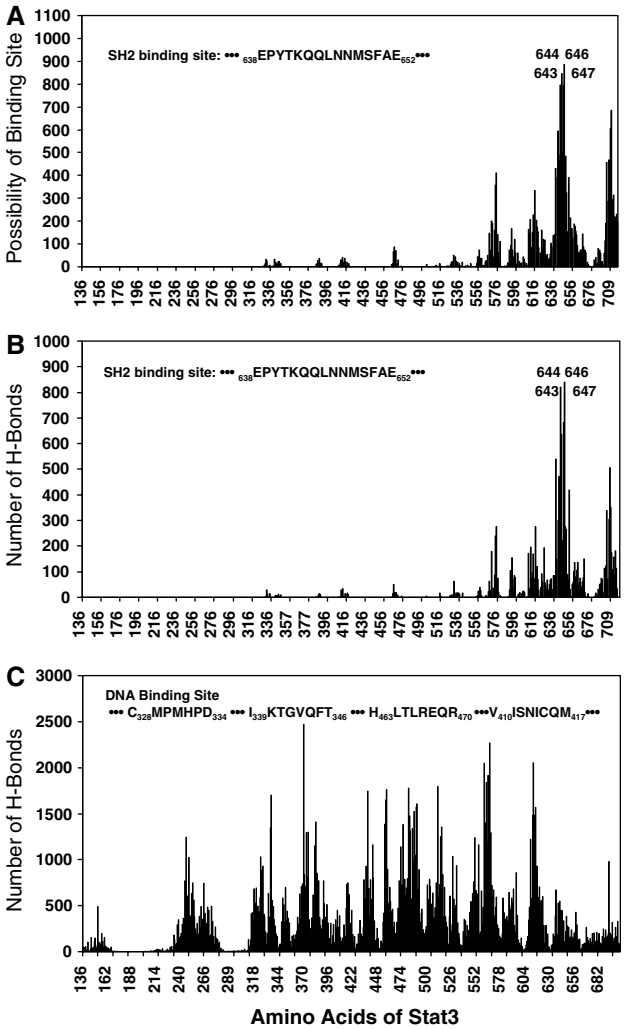

Fig. 2 The H-bonds distibution on amino aicds of Stat3. (**a**) Plot of possibility versus amino acids of Stat3 showed the possible T40214 binding site location. (**b**) H-bond distribution (the number of H-bonds *versus* amino acids of Stat3) after docking T40214 into p-Stat3 dimer 1000 times; the H-bonds predominantly occurred in the area from E638 to E652. (**c**) The H-bond distribution after docking the duplex DNA into p-Stat3 dimer 1000 times; H-bonds randomly distribute on amino acids of Stat3, and the distribution on residues of DNA-binding site (•••C_{328}MPMHPD$_{334}$••• I_{339}KTGVQFT$_{346}$•••H_{410} LTLREQR$_{417}$•••V_{463}ISNICQM$_{470}$•••) is 5%

(residues 136–716) as receptor. The *Hex* docking was restricted to primary binding site determined by both the GRAMM docking and the H-bond analysis. Starting from the lowest energy geometry obtained from GRAMM docking, we scanned a total of 6,718,464 orientations with *Hex* docking program to refine the binding model. The best 512 orientations were collected and clustered according to the strategies as described in Materials and methods. Based upon RMS deviation, 39 different docking models were identified through clustering. Then the best five 3D models were selected to be potential binding models for further energy optimization. All of five 3D models adopted similar

orientation after the energy optimization. The final 3D model (shown in Fig. 3a) was determined with these criteria: the lowest binding energy, the most H-bond formation, favored polar/polar contacts, shape match, and acceptable charge complementarity.

The 3D model (Fig. 3a) indicated that T40214 extends into a channel in SH2 domain of Stat3 dimer, which is formed by two pairs of residues Q643 and N646 belonging to monomer A and B, respectively. The G5 residue of T40214 forms six H-bonds with residues Q643, N646, and N647, and the other residues of T40214 such as G2, G3, and C12 also form H-bonds with amino acids T641, K642, and Q643 of p-Stat3 dimer. The binding pocket for DNA duplex in Stat3 dimer was showed in Fig. 3b. Superimposing complex T40214/p-Stat3 dimer on complex DNA/p-Stat3 dimer together demonstrated an overlay between T40214 and DNA duplex (Fig. 3c). The overlay suggested that T40214 blocks DNA duplex binding to p-Stat3 dimer once it binds in SH2 domain, which was consistent with experimental observation (Lane 4 Fig. 1c).

In order to investigate whether the DNA duplex can bind to Stat3 complex with T40214, we docked the DNA duplex into p-Stat3 dimer with bound T40214. The histogram showed that the H-bonds formed between DNA duplex and the complex of p-Stat3 dimer/T40214 have no predominant distribution (Fig. 2c). The possibilities of H-bond formed with the residues in DNA-binding site of the complex [18] is only 5%, suggesting that it is difficult for the duplex DNA to bind to Stat3 once T40214 occupies the binding site in SH2 domain of Stat3. Therefore, T40214 inhibits Stat3 activation by blocking DNA duplex binding within p-Stat3 dimer.

The mechanism of T40214 selectively targeting p-Stat3 dimer

Stat3 has been identified to be an important molecular target for cancer therapy since it participates in oncogenesis through the up-regulation of genes encoding apoptosis inhibitors, cell-cycle regulators, and inducers of angiogenesis. Stat1, which acts in a pro-apoptotic and anti-proliferative manner, seems to be a tumor suppressor; and its functions are contrary to Stat3 [17]. Thus, the selectively targeting Stat3 rather than Stat1 is a key factor in the design of a more potent and lower side-effect anti-cancer agent. Stat3 and Stat1 have similar function domains as shown in Fig. 4a. Sequence alignment indicated that Stat1 and Stat3 show 51%, 60% and 66% identity in full length, SH2 domain and DNA-binding domain, respectively (alignment was shown in Fig. 4b). The phosphorylated Tyr705 and DNA binding site are usually considered to be potential binding pockets for the design of Stat3 inhibitor.

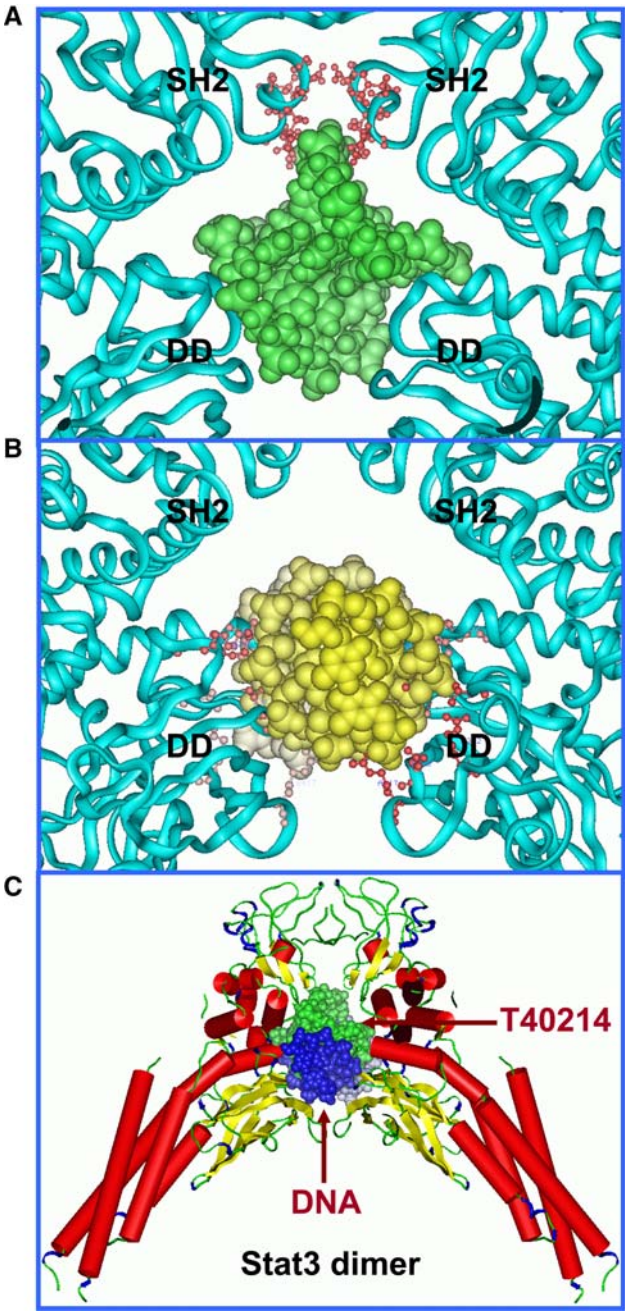

Fig. 3 The mechanism of GQ-ODN T40214 inhibiting Stat3**.** (**a**) The 3D model of complex T40214/p-Stat3 dimer; the residues of Stat3 forming H-bonds with T40214 were colored in red and displayed in ball-and-stick style. (**b**) Interaction between p-Stat3 dimer and the duplex DNA, the residues of Stat3 forming H-bonds with the duplex DNA were colored in red and displayed in ball-and-stick style. (**c**) The 3D strcture of Stat3 dimer superimposing with GQ-ODN T40214 (in green) and bound DNA duplex (in blue)

However, designing selective Stat3 inhibitor based on these sites is very challenging because the residues in these binding sites are highly conserved. Figure 5a listed binding site residues for p-Tyr701 of Stat1 and p-Tyr705 of Stat3 and the residues are virtually identical except

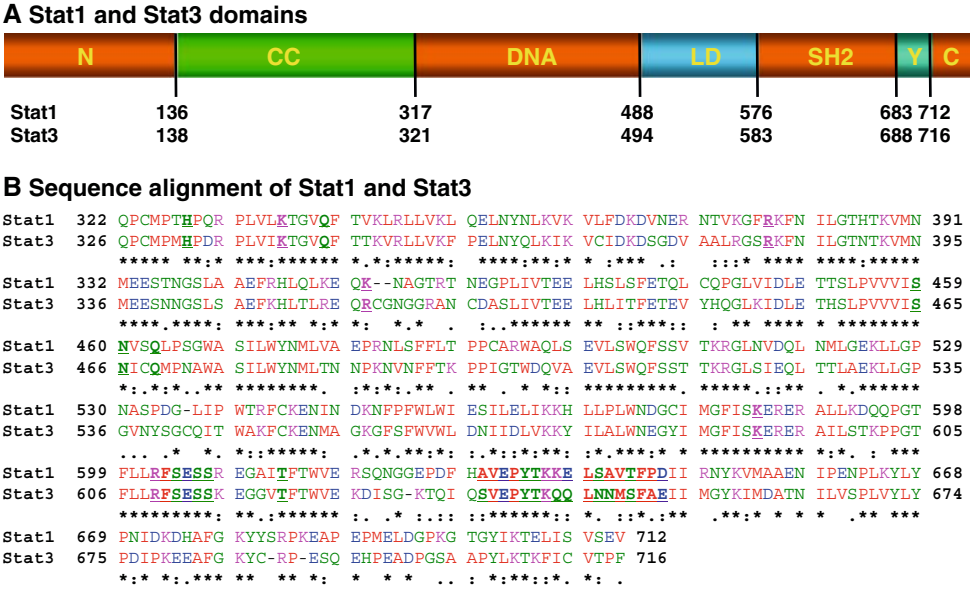

Fig. 4 The partial sequences of Stat1 and Stat3. (**a**) Function domain and amino acid regions in Stat1 and Stat3 core structure; "N" signifies the N-terminal domain, "CC" is the coiled-coil domain, "DNA" is the DNA-binding domain, "LD" is the linking domain, "SH2" is the SH2 domain, "Y" is the conserved tyrosine domain, and "C" is the carboxyl terminal domain; (**b**) core structure sequence alignment for Stat1 and Stat3. "*" indicates that the residues are identical in both sequences, ":" signifies conserved substitutions, and "." signifies semi-conserved substitutions, respectively

one residue S636 (A630 for Stat1). The superimposed 3D structures showed that the RMS deviation of residues in these two binding sites is only 0.49 Å (Fig. 5a). The key residues in DNA binding site are also highly conserved and the residues are virtually identical except R417 (K413 for Stat1). The superimposed 3D structures showed that the RMS deviation of the residues in DNA binding site is only 0.55 Å (Fig. 5b). These comparisons indicated that it might be difficult to design a small and selective Stat3 inhibitor due to the two highly conserved binding sites.

Our previous results have demonstrated that T40214 selectively targets Stat3 dimer [26, 27]. T40214 strongly inhibits the DNA-binding activity of Stat3 at $IC_{50} = 5$ μM, while 50% inhibition of Stat1 DNA-binding activity was not achieved in the concentration up to 142 μM, indicating that selectivity of T40214 is more than 30-fold. In order to design novel and selective Stat3 inhibitor, we employed several computational approaches to investigate the nature of T40214 selectively inhibiting DNA-binding activity of Stat3. Usually, inhibitor selectively targeting to one of family proteins is based on its different sequence and conformation in their active sites. Our docking results showed that T40214 binding site in Stat1 dimer is only 43% identity to that in Stat3 dimer, and the sequences of the binding site residues of Stat1 and Stat3 were aligned in Fig. 5c. The alignment indicated the key residues involving in the binding of T40214 to p-Stat3 dimer are different from the corresponding residues in p-Stat1 dimer. The residues in Stat3 are Q643, Q644, N646 and N647 but the corresponding residues in Stat1 are K637, E638, S640, and A641. The 3D structures of the two binding sites are also different. In p-Stat1 dimer, the side-chain of K637 (with positive charges) is in close proximity to hydroxyl group of S640 and the distance between K637:Nζ of one monomer and S640:O of another is about 3.89 Å. This short distance will induce a strong polar interaction between these two residues, which can pull the two pair residues closer and hold the two SH2 domains together. Therefore this local conformation will block T40214 interact with residues inside SH2 domains of Stat1. However, in p-Stat3 dimer, the paired residues of Q643 and N646 repulse each other due to their negatively charged polar side chains. This repulsion interaction resulted in an open space channel in its SH2 domain. The distance of Q643:Cδ of one monomer to N646:Cγ of another is about 7.15 Å. The channel is favorable for the G5 phosphate group of T40214 to extend to the SH2 domain and then form strong interaction with the inside residues. The 3D models indicated that T40214 deeply extends into SH2 domain of Stat3 dimer and form six H-bonds with residues Q643, N646, and N647, however, T40214 cannot binding in SH2 domain of Stat1 dimer due to no open space for T40214 to enter the SH domain of Stat1 dimer. The two binding structures were showed in molecular surface graphics (Fig. 6). The computational results suggested that the mechanism for T40214 to selectively inhibit Stat3 but not Stat1 is based on their 3D structure of SH2 domains. T40214 forms H-bonds with SH2 domain of Stat3 dimer, so that T40214 will stay in the binding space to block DNA duplex binding interaction. However, T40214 cannot enter into SH2 domain of Stat1 dimer to form H-bonds with the key residues in SH2 domain, thus, T40214 could not stay there to block Stat1 activity.

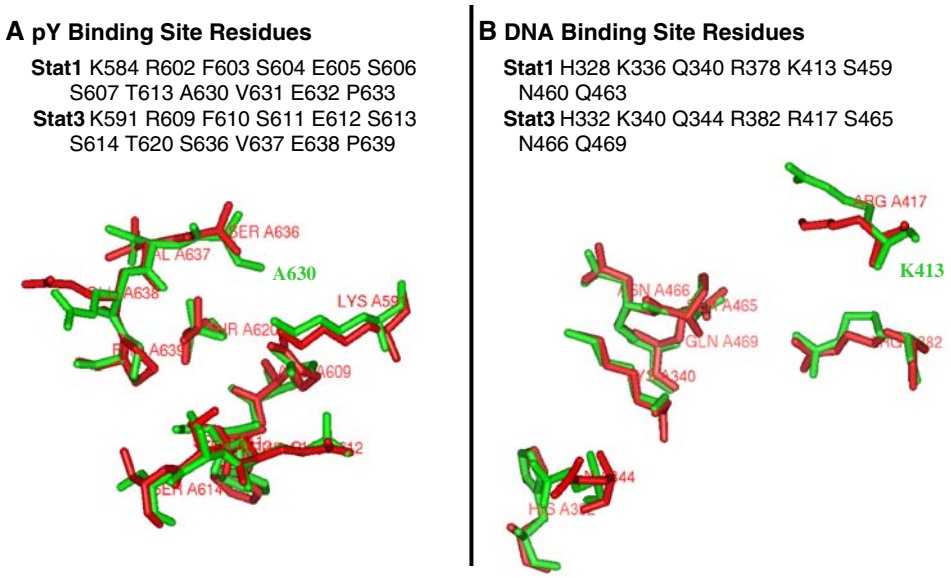

Fig. 5 The molecular simulation results for Stat3 and Stat1. (**a**) Sequence alignment and superposition of residues in binding site for pY701 of Stat1 and pY705 of Stat3; (**b**) sequence alignment and superposition of residues in binding site for Stat1 and Stat3 DNA binding; (**c**) the structure comparison of the binding sites in SH2 domains of Stat1 (left panel) and Stat3 (right panel) dimers (see details in text)

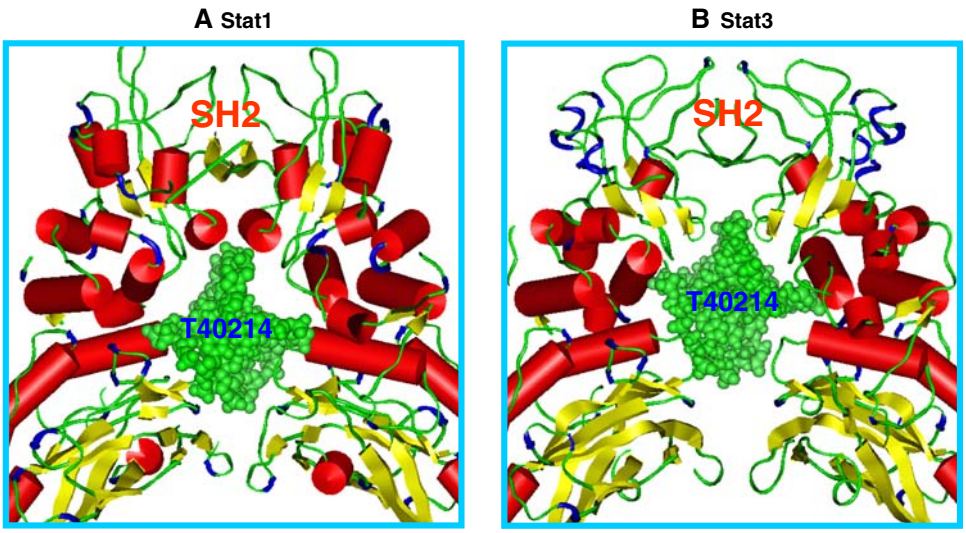

Fig. 6 Structures of GQ-ODN T40214 targeting Stat1 and Stat3. (**a**) Surface display of binding interaction between Stat1 dimer and T40214; (**b**) surface display of binding interaction between Stat3 dimer and T40214. T40214 selectively inhibits DNA-binding activity of Stat3 but not Stat1 due to different interaction in SH2 domain

Conclusions

Our previous results have demonstrated that GQ-ODN T40214 is a potent anti-cancer agent by selectively inhibiting DNA-binding activity of Stat3. In order to understand the mechanism of T40214 as a selective Stat3 inhibitor, we established a 3D model for T40214/p-Stat3 dimer by employing several computer-based approaches. Our computational results demonstrated that T40214 inhibits Stat3 activity through directly blocking DNA binding because it destabilizes Stat3 dimer complex with DNA. By comparing with the sequences and 3D structures between p-Stat3 and p-Stat1, we found that the local structures of T40214 binding site is slightly different between Stat3 dimer and Stat1 dimer. The difference on SH2 domains between Stat1 and Stat3 was proposed as a main factor for GQ-ODN T40214 selectively inhibiting Stat3 activation. These results provide a useful platform for rational drug design of Stat3 inhibitors.

Acknowledgments The authors wish to thank Yidong Li, who contributed to this study by providing the EMSA results. This project was supported by the following grants: CA104035 (NIH) and competitive award from Prostate Cancer Foundation. In addition, Dr. Zhu received support through NIH training grant T32 DK60445.

References

1. Darnell JE (1997) Science 277:1630
2. Bromberg J, Darnell JE (2000) Oncogene 19:2468
3. Darnell JE (2002) Nat Rev Cancer 2:740
4. Heinrich PC, Behrmann I, Muller-Newen G, Schaper F, Graeve L (1998) Biochem J 334(Pt 2):297
5. Hirano T, Ishihara K, Hibi M (2000) Oncogene 19:2548
6. Takeda K, Akira S (2000) Cytokine Growth Factor Rev 11:199
7. Lutticken C, Wegenka UM, Yuan J, Buschmann J, Schindler C, Ziemiecki A, Harpur AG, Wilks AF, Yasukawa K, Taga T et al (1994) Science 263:89
8. Raz R, Durbin JE, Levy DE (1994) J Biol Chem 269:24391
9. Wegenka UM, Lutticken C, Buschmann J, Yuan J, Lottspeich F, Muller-Esterl W, Schindler C, Roeb E, Heinrich PC, Horn F (1994) Mol Cell Biol 14:3186
10. Zhong Z, Wen Z, Darnell JE Jr (1994) Science 264:95
11. Catlett-Falcone R, Landowski TH, Oshiro MM, Turkson J, Levitzki A, Savino R, Ciliberto G, Moscinski L, Fernandez-Luna JL, Nunez G, Dalton WS, Jove R (1999) Immunity 10:105
12. Grandis JR, Drenning SD, Chakraborty A, Zhou MY, Zeng Q, Pitt AS, Tweardy DJ (1998) J Clin Invest 102:1385
13. Bowman T, Garcia R, Turkson J, Jove R (2000) Oncogene 19:2474
14. Buettner R, Mora LB, Jove R (2002) Clin Cancer Res 8:945
15. Silvennoinen O, Schindler C, Schlessinger J, Levy DE (1993) Science 261:1736
16. Darnell JE Jr, Kerr IM, Stark GR (1994) Science 264:1415
17. Levy DE, Darnell JE Jr (2002) Nat Rev Mol Cell Biol 3:651
18. Becker S, Groner B, Muller CW (1998) Nature 394:145
19. Chen X, Vinkemeier U, Zhao Y, Jeruzalmi D, Darnell JE Jr, Kuriyan J (1998) Cell 93:827
20. Xu X, Sun YL, Hoey T (1996) Science 273:794
21. Horvath CM, Wen Z, Darnell JE Jr (1995) Genes Dev 9:984
22. Shuai K, Horvath CM, Huang LH, Qureshi SA, Cowburn D, Darnell JE Jr (1994) Cell 76:821
23. Jing N, Tweardy DJ (2005) Anticancer Drugs 16:601
24. Jing N, Li Y, Xu X, Sha W, Li P, Feng L, Tweardy DJ (2003) DNA Cell Biol 22:685
25. Weerasinghe P, Garcia GE, Zhu Q, Yuan P, Feng L, Mao L, Jing N (2007) Int J Oncol 31:129
26. Jing N, Zhu Q, Yuan P, Li Y, Mao L, Tweardy DJ (2006) Mol Cancer Ther 5:279
27. Jing N, Li Y, Xiong W, Sha W, Jing L, Tweardy DJ (2004) Cancer Res 64:6603
28. Grandis JR, Drenning SD, Zeng Q, Watkins SC, Melhem MF, Endo S, Johnson DE, Huang L, He Y, Kim JD (2000) Proc Natl Acad Sci USA 97:4227
29. Ramana CV, Grammatikakis N, Chernov M, Nguyen H, Goh KC, Williams BR, Stark GR (2000) Embo J 19:263
30. Yu H, Jove R (2004) Nat Rev Cancer 4:97
31. Jing N, Hogan ME (1998) J Biol Chem 273:34992
32. Pearlmann DA, Case DA, Caldwell JW, Ross WS, Cheatham TE, III DeBolt S, Ferguson D, Seibel G, Kollman P (1995) Comp Phys Commun 91:1
33. Berman HM, Westbrook J, Feng Z, Gilliland G, Bhat TN, Weissig H, Shindyalov IN, Bourne PE (2000) Nucleic Acids Res 28:235
34. Berman HM, Olson WK, Beveridge DL, Westbrook J, Gelbin A, Demeny T, Hsieh SH, Srinivasan AR, Schneider B (1992) Biophys J 63:751
35. Ritchie DW, Kemp GJ (2000) Proteins 39:178
36. Boeckmann B, Bairoch A, Apweiler R, Blatter MC, Estreicher A, Gasteiger E, Martin MJ, Michoud K, O'Donovan C, Phan I, Pilbout S, Schneider M (2003) Nucleic Acids Res 31:365
37. Thompson JD, Higgins DG, Gibson TJ (1994) Nucleic Acids Res 22:4673
38. Neculai D, Neculai AM, Verrier S, Straub K, Klumpp K, Pfitzner E, Becker S (2005) J Biol Chem 280:40782
39. Mao X, Ren Z, Parker GN, Sondermann H, Pastorello MA, Wang W, McMurray JS, Demeler B, Darnell JE Jr, Chen X (2005) Mol Cell 17:761
40. Soler-Lopez M, Petosa C, Fukuzawa M, Ravelli R, Williams JG, Muller CW (2004) Mol Cell 13:791